

# Modular Vaccine Design Using Carrier-Free Capsules Assembled from Polyionic Immune Signals

Yu-Chieh Chiu,<sup>†</sup> Joshua M. Gammon,<sup>†</sup> James I. Andorko,<sup>†</sup> Lisa H. Tostanoski,<sup>†</sup> and Christopher M. Jewell<sup>\*,†,‡,§</sup>

<sup>†</sup>Fischell Department of Bioengineering, University of Maryland, 2212 Jeong H. Kim Building, College Park, Maryland 20742, United States

<sup>‡</sup>Department of Microbiology and Immunology, University of Maryland Medical School, 685 West Baltimore Street, HSF-I Suite 380, Baltimore, Maryland 21201, United States

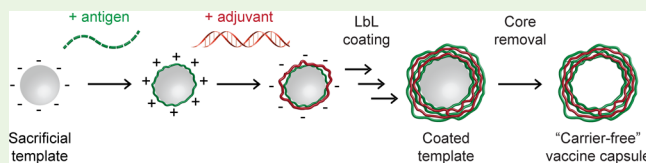
<sup>§</sup>Marlene and Stewart Greenebaum Cancer Center, 22 South Greene Street, Suite N9E17, Baltimore, Maryland 21201, United States

## S Supporting Information

**ABSTRACT:** New vaccine adjuvants that direct immune cells toward specific fates could support more potent and selective options for diseases spanning infection to cancer. However, the empirical nature of vaccines and the complexity of many formulations has hindered design of well-defined and easily characterized vaccines. We hypothesized that nanostructured capsules assembled entirely from polyionic immune signals

might support a platform for simple, modular vaccines. These immune-polyelectrolyte (iPEM) capsules offer a high signal density, selectively expand T cells in mice, and drive functional responses during tumor challenge. iPEMs incorporating clinically relevant antigens could improve vaccine definition and support more programmable control over immunity.

**KEYWORDS:** rational design, immunology, self-assembly, vaccine, polyelectrolyte multilayer



Despite the tremendous clinical success of vaccines, the complexity of some of the most pervasive diseases continues to create challenges for new vaccines. For example, HIV virus is able to evade immune clearance by rapid mutation and concealment in the mucosa, and cancerous tissues actively suppress tumor-destructive immune cells.<sup>1–3</sup> The ability to rationally design vaccines or immunotherapies that elicit immune responses with specific characteristics (e.g., phenotypes, tissue homing, memory) could improve both the efficacy and robustness of these technologies. Improved vaccine adjuvants could help realize this vision by eliciting responses that are potent, but that also exhibit particular features. A major hurdle to this goal is the complex composition (e.g., carriers, excipients, adjuvants, antigens) that makes characterizing and testing the multitude of new vaccine candidates empirical and economically infeasible.<sup>4</sup> Thus, there is a need for simpler, more modular technologies to support a new generation of human vaccine adjuvants.

Biomaterials have been explored to improve adjuvant performance because these materials offer controlled release, codelivery of multiple cargos, and targeting to sites such as lymph nodes—tissues that coordinate adaptive immunity.<sup>5–8</sup> Although traditionally viewed as passive carriers, recent studies have led to a revelation that many ubiquitous polymeric vaccine carriers activate inflammatory pathways even in the absence of other antigens or adjuvants. Examples of both degradable and nondegradable materials have been reported in this context, including poly(lactide-co-glycolide), poly(styrene), chitosan,

and hyaluronic acid.<sup>9–12</sup> Thus, although polymeric materials offer great potential for new vaccines, the intrinsic immune characteristics can hinder rational vaccine design and translation because the role of the carrier itself may alter how other vaccine components or signals (e.g., antigens, adjuvants) are processed.

To address the challenges above, we identified three design features that would enable more programmable vaccines: (i) modularity to assemble different types of antigens or adjuvants at a high signal density, (ii) defined compositions that eliminate excess carrier components, and (iii) simple, low-energy manufacturing processes that do not require homogenization or sonication. Polyelectrolyte multilayers (PEMs) are self-assembled structures that offer many of these features. These films are formed through electrostatic interactions during a layer-by-layer (LbL) deposition process.<sup>13–16</sup> PEMs assembled from a range of polymers—such as dextran sulfates, poly( $\beta$ -amino esters), or poly(L-glutamic acids)—have been used to enhance vaccination in flu, cancer, and HIV by injecting particles or capsules that encapsulate or adsorb vaccine components with the polymers.<sup>17–24</sup> In comparison to our recent work with PEMs assembled on gold nanoparticles,<sup>25</sup> here we present a platform for simplifying vaccine design and evaluation by electrostatically assembling stable vaccine

**Received:** September 1, 2015

**Accepted:** October 30, 2015

**Published:** November 2, 2015

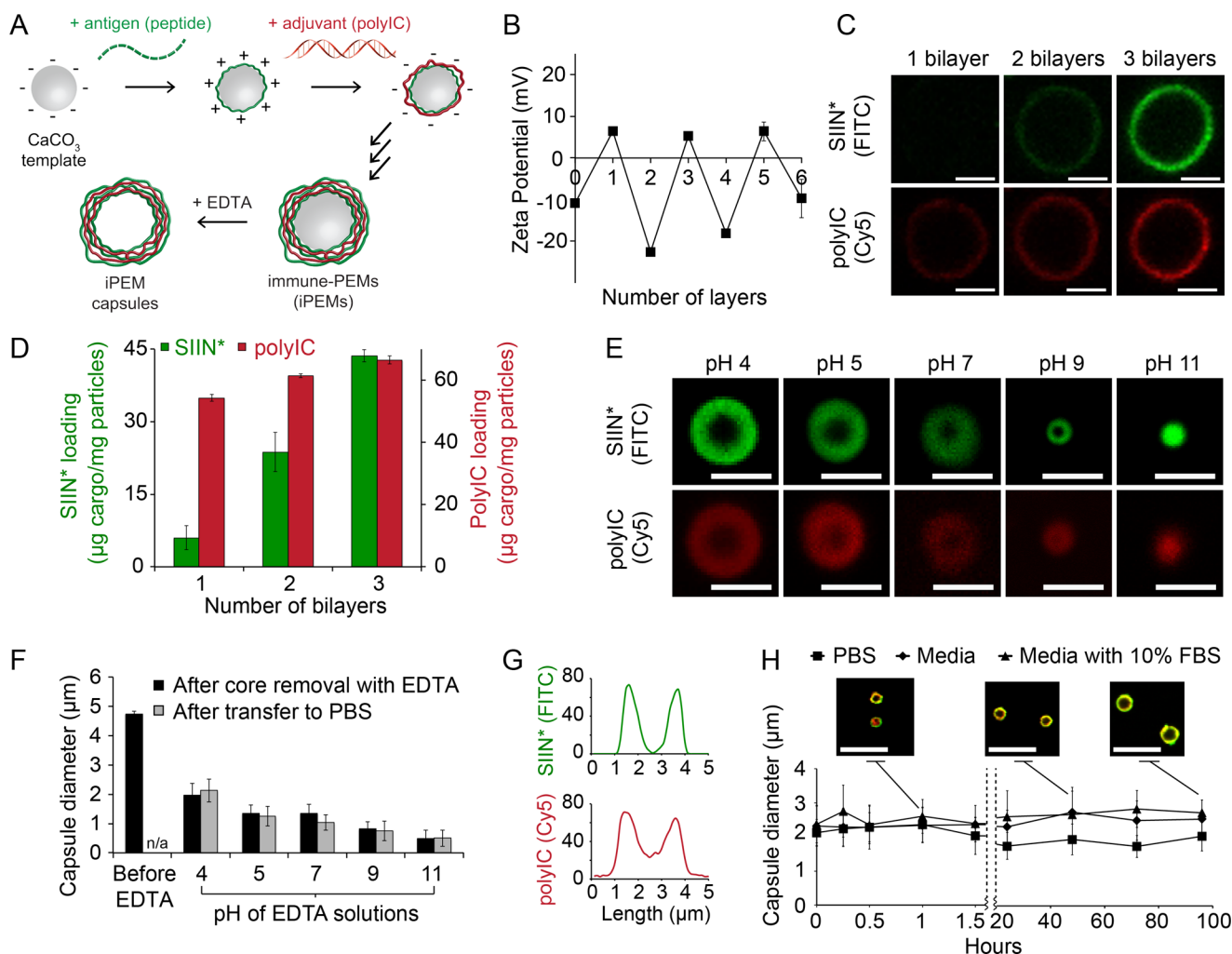


**Figure 1.** iPEM capsules are stable and exhibit sizes that are a function of pH. (A) Schematic representation of iPEM capsule synthesis using antigens and adjuvants. (B) Zeta potential measurements indicating charge inversion as each antigen or adjuvant layer is adsorbed during iPEM synthesis. (C) Confocal microscopy images and (D) cargo loading during assembly of (SIIN\*/polyIC)<sub>3</sub> on CaCO<sub>3</sub> templates. (E) Confocal microscopy images and (F) diameter of iPEM capsules formed following removal of the core with EDTA at the indicated pH values (black bars), and after subsequent transfer to PBS (gray bars). (G) Fluorescent intensity distributions of SIIN\* (FITC) and polyIC (Cy5) across a cross-section of a representative capsule formed by EDTA treatment at pH 4. (H) Stability of iPEM capsules during incubation at 37 °C in PBS, media, or media with 10% FBS. The inset shows images of iPEM capsules during incubation in media with 10% FBS for 1, 48, and 96 h. Values for all panels represent the mean ± standard deviation. Scale bars: (C, E) 2.5 μm; (H) 10 μm.

capsules solely from immune signals. The elimination of supports, synthetic polymers, and other carrier components distinguishes our work from all past reports. These immune-PEM (“iPEM”) capsules mimic many features of biomaterials (e.g., tunable sizes, codelivery), enhance vaccination by increasing the density and programmability of immune signals, and eliminate components that can exhibit poorly defined immunogenic characteristics (e.g., synthetic materials).

iPEM capsules are assembled through alternate deposition of peptide antigens and toll-like receptor agonists (TLRAs) as adjuvants (Figure 1A). This process is all aqueous and does not require heating, cooling, or mixing. iPEMs are built on a sacrificial core in an LbL manner and comprise polyinosinic-polycytidylic acid (polyIC)—an immunostimulatory double stranded RNA (i.e., TLR3 agonist)—and antigenic peptides from a common model antigen, ovalbumin (SIINFEKL). In this system, the TLRAs serve as potent molecular adjuvants and polyanionic film components, while SIINFEKL modified with nona-arginine (SIIN\*) at the carboxy-terminus serves as the

antigen and a cationic film component. To design iPEM capsules formed entirely from these immune signals, we first assembled iPEMs on 5 μm CaCO<sub>3</sub> sacrificial cores. Film assembly was confirmed by the oscillation of zeta potentials between positive and negative values as each respective layer of SIIN\* and polyIC was deposited (Figure 1B). Confocal microscopy further confirmed film growth, with increasing fluorescence corresponding to SIIN\* and polyIC as the bilayer number increased (Figure 1C). These images also revealed polyIC and SIIN\* were juxtaposed in the film structure, as indicated by colocalization of the fluorescent signal for each component (Figure 1C). Control studies confirmed fluorescent signals from antigen and adjuvant could be independently visualized (Figure S1). Cargo loading was also tunable by varying the number of layers deposited, with UV/vis spectroscopy and fluorimetry indicating loading of ~44 μg of SIIN\*/mg of particles and ~67 μg of polyIC/mg of particles during assembly of (SIIN\*/polyIC)<sub>3</sub> (Figure 1D).

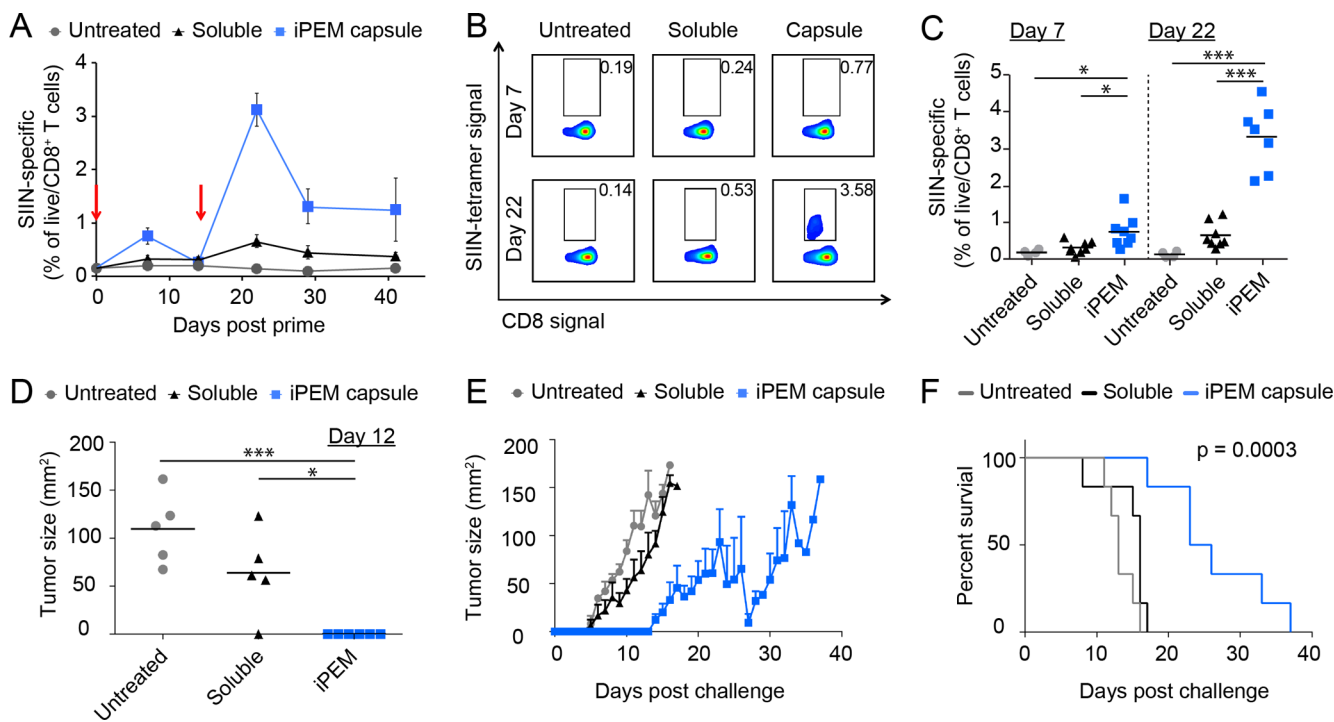


**Figure 2.** Immunization with iPEM capsules promotes synergistic expansion of antigen specific CD8<sup>+</sup> T cells by enhancing DC function. (A–C) C57BL/6 mice were immunized intradermally with equivalent doses of antigen and adjuvant formulated in iPEM capsules or using a mixture of free components at day 0 and day 15 (red arrows). (A) Quantification of SIINFEKL-specific CD8<sup>+</sup> T cells in peripheral blood measured over 41 days using MHC-I SIINFEKL tetramer. (B) Representative scatter plots and (C) mean frequencies of live/CD8<sup>+</sup>/SIINFEKL<sup>+</sup> cells in peripheral blood at the peak of primary (day 7) and recall (day 22) responses following immunization. (D) Tumor size on day 12 after a challenge with  $1 \times 10^6$  B16-OVA cells administered on day 36. Mice were vaccinated with the indicated formulations on days 0, 15, and 28. (E) Tumor burden over time in mice immunized as described in D. (F) Survival curves demonstrating immunization with iPEM capsules prolongs survival after tumor challenge. Values for all panels indicate the mean  $\pm$  s.e.m. and are representative of 2–3 experiments using  $N = 4$  for groups of naïve mice,  $N = 8$  mice/group for immunization studies,  $N = 6$  mice/group for tumor studies. Statistics are indicated for all significant comparisons using criteria of \*  $p \leq 0.05$ ; \*\*  $p \leq 0.01$ ; \*\*\*  $p \leq 0.001$ .

To form support-free iPEM capsules, we removed CaCO<sub>3</sub> templates with ethylenediaminetetraacetic acid (EDTA), leaving (SIIN\*/polyIC)<sub>3</sub> capsules composed entirely of antigen and adjuvant (Figure 1A). Capsule size could be tuned by varying the pH of the EDTA solution used for core removal, with an inverse relationship between capsule size and increasing EDTA pH. Cores removed with EDTA at a pH of 4 resulted in capsules with microscale diameters ( $\sim 2.2 \mu\text{m}$ ), whereas capsules exhibited nanoscale diameters ( $\sim 700 \text{ nm}$ ) when cores were removed with EDTA at higher pH values (Figure 1E, F). Past fundamental studies have shown that polyelectrolyte capsule size and stability are relatively constant over intermediate pH ranges where electrostatic forces are dominant.<sup>26</sup> At more acidic or more basic conditions outside this range, hydrophobic forces and surface tension become dominant as excess charge of one polyion is no longer fully compensated. These effects minimize capsule size, and at extreme pH values, can lead to collapse. Our results with iPEMs are in agreement with this theory, as we observed stable capsules from pH 4–9, but collapsed capsules at pH 11 as uncompensated charge on polyIC increased due to decreasing cationic charge on SIIN\* at this very basic pH (Figure 1E, F). We also discovered that the sizes of iPEM nanocapsules and microcapsules were maintained upon transfer to PBS after removal of the core (Figure 1F, gray bars), confirming a robust approach for tuning capsule diameter. We selected capsules formed with EDTA at pH 4 for further study and confirmed colocalization of antigen and adjuvant in the capsule shell after

core removal by pixel intensity analysis of confocal microscopy line scans (Figure 1G). Incubation of iPEM capsules in PBS, media, or media supplemented with 10% FBS confirmed capsules were stable for at least 96 h (Figure 1H). Of particular note, iPEM capsules incubated in complete media exhibited only a slight increase in size, with an initial mean diameter of  $2.4 \mu\text{m}$  compared to  $2.7 \mu\text{m}$  after 96 h (Figure 1H). These data confirm that stable iPEM capsules can be assembled from peptide antigens and adjuvants at different length scales and with control over the composition of the capsules. This is an attractive feature for vaccination, for example, to allow design of nanoscale capsules that promote passive drainage to lymph nodes, or of larger capsules that are readily internalized by peripheral antigen presenting cells.<sup>7,27</sup>

We next assessed the adjuvant effects of iPEM capsules by measuring TLR activation and iPEM-triggered secretion of inflammatory cytokines. iPEM capsules were prepared using SIIN\* and either polyIC (TLR3 agonist) or a nonimmunogenic oligonucleotide (ODN) (Figure S2). Reporter cells treated with (SIIN\*/polyIC)<sub>3</sub> iPEM capsules displayed efficient activation of TLR3, whereas (SIIN\*/ODN)<sub>3</sub> capsules did not activate TLR3 signaling. In line with these findings, iPEM capsules incubated with primary dendritic cells (DC) induced pro-inflammatory cytokines—including IFN- $\gamma$  and IL-6—at levels that were significantly higher than cells treated with equivalent doses of free polyIC, peptide, or peptide and polyIC (Figure S3). Together, these results confirm that iPEM capsules

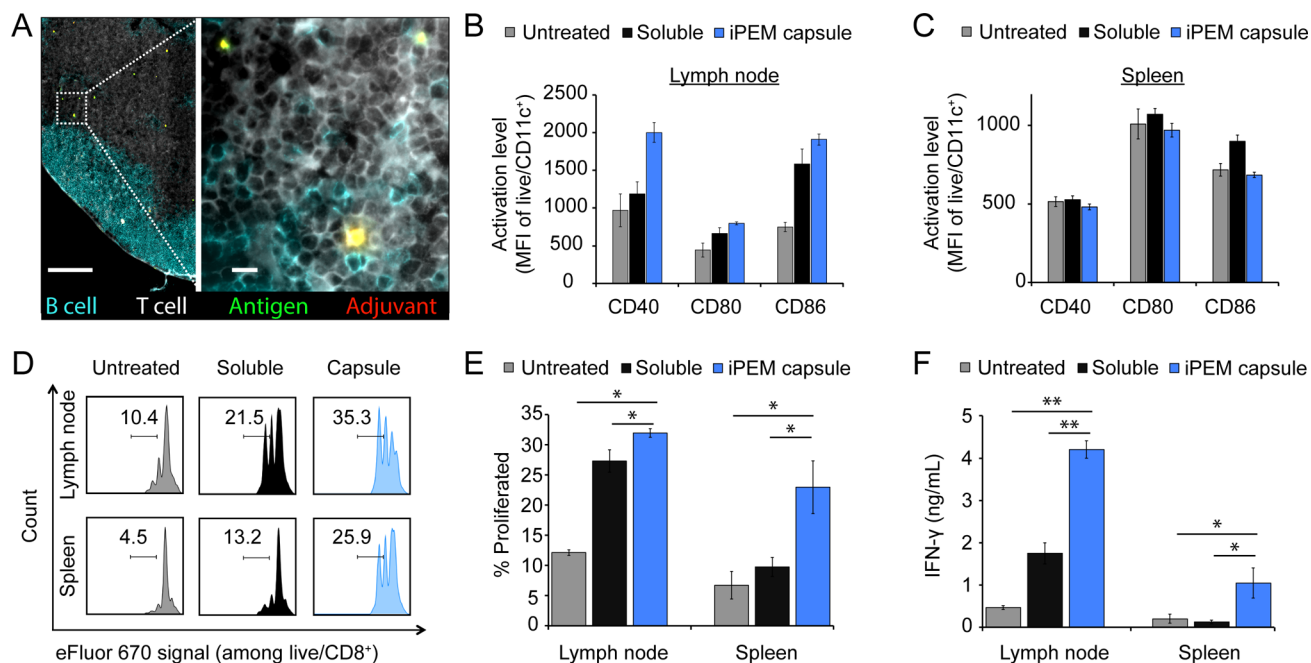


**Figure 3.** (A) Immunohistochemical staining of draining lymph node 3 days after intradermal immunization with the indicated vaccine (T cells (CD3), white; B cells (B220), blue; SIIN<sup>\*</sup>, green; polyIC, red). Scale bars are 200 and 10  $\mu$ m (inlay). (B–F) DCs from (B) draining lymph nodes and (C) spleens were isolated and evaluated for activation using expression of CD40, CD80, and CD86. (D) Histograms and (E) mean frequencies showing the proliferation of labeled, SIIN-specific CD8<sup>+</sup> T cells cocultured for 48 h with DCs from lymph nodes and spleens prepared as in B and C. (F) Secretion of IFN- $\gamma$  in DC and T cell cocultures as in B and C. Values for all panels indicate the mean  $\pm$  s.e.m and are representative of 2–3 experiments using  $N = 4$  for groups of naive mice, and  $N = 8$  mice/group for immunization studies. Statistics are indicated for all significant comparisons using criteria of \*  $p \leq 0.05$ ; \*\*  $p \leq 0.01$ ; \*\*\*  $p \leq 0.001$ .

activate pathogen detection and response pathways that play a key role in the generation of adaptive T cell immunity.

To assess iPEM capsules as a vaccination platform, we immunized mice intradermally with iPEMs or equivalent doses of antigen and adjuvant in free form. One week after injection, iPEMs elicited a modest but significant increase in circulating CD8<sup>+</sup> T cells specific for the SIINFEKL antigen used to assemble iPEMs (Figure 2A). Following a booster injection on day 15, mice exhibited potent recall responses, with up to 4.6% of circulating CD8<sup>+</sup> T cells primed against SIINFEKL (Figure 2A–C). The mean frequency observed with iPEM capsules (3.1%) represented a 4.5-fold enhancement over the level (0.7%) observed in mice treated and boosted with the admixed formulations of antigen and polyIC (Figure 2A–C). The higher SIINFEKL-specific T cell levels associated with iPEM immunization were also durable until the conclusion of the study on day 41.

To determine if these enhanced T cell responses translated to functional immunity, we challenged immunized mice with an aggressive dose of  $1 \times 10^6$  B16 tumor cells expressing OVA. Compared with mice receiving admixed vaccines, iPEMs delayed the formation of palpable tumors (Figure 2D), and dramatically slowed tumor growth (Figure 2E). These effects drove a statistically significant increase in median survival, with a value of 25 days for mice immunized with iPEM capsules, and 16 days and 13 days for soluble formulations and unimmunized mice, respectively (Figure 2F). Thus, iPEMs enhance antigen-specific CD8<sup>+</sup> T cell primary and recall responses in a manner that translates to significant protection during an aggressive tumor challenge.

To investigate the mechanisms behind the enhanced immunogenicity of iPEMs compared with mixtures of peptide

and adjuvant, we immunized groups of mice with iPEM capsules or the free form of the vaccine. After 3 days, spleens and lymph nodes were harvested. Immunofluorescent staining at this time revealed iPEMs distributed throughout the cortex of the lymph node (Figure 3A). Antigen and adjuvant were colocalized, as indicated by the yellow signal resulting from overlapping red (polyIC) and green (SIIN<sup>\*</sup>) fluorescence. This ability to codeliver cargo to secondary lymph organs is an attractive feature for vaccination and immunotherapy. Next, DC activation was assessed quantitatively in these tissues using flow cytometry. Compared with untreated groups or groups immunized with soluble vaccine, mice immunized with iPEM capsules exhibited upregulation of surface activation and costimulatory markers (e.g., CD40, CD80, and CD86) in draining lymph nodes (Figure 3B; Figure S4), but not in spleens (Figure 3C; Figure S5). This finding suggests that iPEM capsules locally enhance the function of DCs sampling the incoming signals from lymphatics (i.e., in draining lymph nodes). In a subsequent study, isolated DCs from identically immunized mice were cocultured with CD8<sup>+</sup> T cells from OT-I mice, a strain in which CD8<sup>+</sup> T cells proliferate upon encounter of SIIN presented via DCs with appropriate costimulatory signals. In these studies, DCs from iPEM capsule-immunized mice drove greater T cell proliferation compared with DCs from mice immunized with simple mixtures of peptide and adjuvant (Figure 3D, E; Figure S6). These effects translated to enhanced cytokine response, with T cells secreting significantly greater IFN- $\gamma$  (Figure 3F).

Throughout our studies, we generally observed that iPEM capsules enhanced the function of DCs (e.g., activation, cytokine secretion) and T cells (e.g., antigen-specific proliferation). These enhancements likely resulted at least in

part from the improved uptake and recognition associated with immune signals in a particulate form.<sup>28,29</sup> Because iPEMs do not require a carrier component, the high density of signals in these structures and the tight colocalization of antigen and adjuvant might be one feature that contributes to the enhanced costimulation and immunogenicity that was observed. Additionally, nona-arginine is a cell penetrating peptide (CPP) that supports cargo internalization, including both antigens and adjuvants.<sup>30</sup> Recent work reveals that intracellular proteases can efficiently process CPPs, and that these moieties can enhance DC function and cross-presentation when antigens are present.<sup>31</sup> These features of CPPs may also contribute to the greater potency of polyIC and peptides in iPEM vaccines compared with free forms of peptide and adjuvant.

The goal of this research is to simplify vaccine composition and synthesis while maintaining useful features of biomaterial carriers (e.g., codelivery of vaccine components, high signal densities, tunable sizes). This is an important idea for the biomaterials and vaccine fields because recent studies demonstrate that many ubiquitous vaccine carriers exhibit intrinsic inflammatory functions. Designing simple, “carrier-free” vaccines provides an opportunity to more clearly understand how each immune component impacts vaccine response, and perhaps, to develop new rational design methodologies that significantly improve the potency and selectivity of future vaccines. Several recent approaches have explored well-controlled synthetic or peptide-based materials to probe or direct immune signaling.<sup>8,32–34</sup> These systems further underscore the potential of modular approaches that support more rational design of vaccines.

From a translational perspective, iPEM capsules offer several attractive features including facile incorporation of different types of antigens or adjuvants, elimination of potential confounding effects from intrinsic immunogenicity of polymers, and cargo loading densities of 100% (compared with typical loadings of 0.5–5% obtained with cargo loaded in polymer particles or matrices).<sup>35,36</sup> Further, iPEM assembly does not require solvents, heating/cooling, synthetic polymers, water-insoluble components, or mixing. Although benchmarking against current adjuvants and integration of clinically relevant antigens will be required as next steps, this platform could help improve the specificity and effectiveness of new vaccines by harnessing immunological building blocks as both nanostructured carriers and as signals that actively direct immune response.

## ■ ASSOCIATED CONTENT

### 📄 Supporting Information

The Supporting Information is available free of charge on the ACS Publications website at DOI: [10.1021/acsbomaterials.5b00375](https://doi.org/10.1021/acsbomaterials.5b00375).

Supplementary methods, TLR3 activation, cytokine production, flow cytometry traces, and mean fluorescent intensities (PDF)

## ■ AUTHOR INFORMATION

### Corresponding Author

\*E-mail: [cmjewell@umd.edu](mailto:cmjewell@umd.edu). Web: [jewell.umd.edu](http://jewell.umd.edu). Phone: 301-405-9628. Fax: 301-405-9953.

### Notes

The authors declare no competing financial interest.

## ■ ACKNOWLEDGMENTS

We acknowledge A. Beaven at the University of Maryland Imaging Core Facility for assistance in confocal microscopy. This work was supported in part by NSF CAREER Award 1351688 and the University of Maryland Division of Research (Tier 1). Y.C.C. is a trainee on NIH Grant T32 CA154274. J.M.G. is a grantee of the Pediatric Oncology Student Training award from Alex's Lemonade Stand Foundation. J.I.A. is a trainee on NIH Grant T32 AI089621 and a Graduate Fellow supported by the American Association of Pharmaceutical Scientists Foundation. L.H.T. is a fellow supported by the NSF Graduate Research Fellowship Program Grant DGE1322106. C.M.J. is a Damon Runyon-Rachleff Innovator supported by the Damon Runyon Foundation, a Young Investigator supported by the Alliance for Cancer Gene Therapy, and a Young Investigator supported by the Melanoma Research Alliance.

## ■ ABBREVIATIONS

CPP, cell penetrating peptide  
DC, dendritic cell  
EDTA, ethylenediaminetetraacetic acid  
iPEM, immune-polyelectrolyte multilayer  
LbL, layer-by-layer  
ODN, nonimmunostimulatory control oligonucleotide  
polyIC, polyinosinic-polycytidylic acid  
SIIN, SIINFELK peptide  
SIIN\*, SIINFELK-R<sub>1</sub> peptide  
TLRa, toll-like receptor agonist

## ■ REFERENCES

- (1) Roush, S. W.; Murphy, T. V. Historical comparisons of morbidity and mortality for vaccine-preventable diseases in the United States. *JAMA* **2007**, *298* (18), 2155–2163.
- (2) Grivennikov, S. I.; Greten, F. R.; Karin, M. Immunity, Inflammation, and Cancer. *Cell* **2010**, *140* (6), 883–899.
- (3) McMichael, A. J.; Borrow, P.; Tomaras, G. D.; Goonetilleke, N.; Haynes, B. F. The immune response during acute HIV-1 infection: clues for vaccine development. *Nat. Rev. Immunol.* **2010**, *10* (1), 11–23.
- (4) Wu, T. Y. H.; Singh, M.; Miller, A. T.; De Gregorio, E.; Doro, F.; D'Oro, U.; Skibinski, D. A. G.; Mbow, M. L.; Bufali, S.; Herman, A. E.; Cortez, A.; Li, Y.; Nayak, B. P.; Tritto, E.; Filippi, C. M.; Otten, G. R.; Brito, L. A.; Monaci, E.; Li, C.; Aprea, S.; Valentini, S.; Calabro, S.; Laera, D.; Brunelli, B.; Caproni, E.; Malyala, P.; Panchal, R. G.; Warren, T. K.; Bavari, S.; O'Hagan, D. T.; Cooke, M. P.; Valiante, N. M. Rational design of small molecules as vaccine adjuvants. *Sci. Transl. Med.* **2014**, *6* (263), 263ra160.
- (5) Hubbell, J. A.; Thomas, S. N.; Swartz, M. A. Materials engineering for immunomodulation. *Nature* **2009**, *462* (7272), 449–460.
- (6) Irvine, D. J.; Swartz, M. A.; Szeto, G. L. Engineering synthetic vaccines using cues from natural immunity. *Nat. Mater.* **2013**, *12* (11), 978–990.
- (7) Andorko, J. I.; Hess, K. L.; Jewell, C. M. Harnessing biomaterials to engineer the lymph node microenvironment for immunity or tolerance. *AAPS J.* **2015**, *17* (2), 323–38.
- (8) Hudalla, G. A.; Sun, T.; Gasiorowski, J. Z.; Han, H. F.; Tian, Y. F.; Chong, A. S.; Collier, J. H. Graded assembly of multiple proteins into supramolecular nanomaterials. *Nat. Mater.* **2014**, *13* (8), 829–836.
- (9) Sharp, F. A.; Ruane, D.; Claass, B.; Creagh, E.; Harris, J.; Malyala, P.; Singh, M.; O'Hagan, D. T.; Petrilli, V.; Tschopp, J.; O'Neill, L. A.; Lavelle, E. C. Uptake of particulate vaccine adjuvants by dendritic cells

activates the NALP3 inflammasome. *Proc. Natl. Acad. Sci. U. S. A.* **2009**, *106* (3), 870–5.

(10) Demento, S. L.; Eisenbarth, S. C.; Foellmer, H. G.; Platt, C.; Caplan, M. J.; Mark Saltzman, W.; Mellman, I.; Ledizet, M.; Fikrig, E.; Flavell, R. A.; Fahmy, T. M. Inflammasome-activating nanoparticles as modular systems for optimizing vaccine efficacy. *Vaccine* **2009**, *27* (23), 3013–21.

(11) Da Silva, C. A.; Chalouni, C.; Williams, A.; Hartl, D.; Lee, C. G.; Elias, J. A. Chitin is a size-dependent regulator of macrophage TNF and IL-10 production. *J. Immunol.* **2009**, *182* (6), 3573–82.

(12) Termeer, C.; Benedix, F.; Sleeman, J.; Fieber, C.; Voith, U.; Ahrens, T.; Miyake, K.; Freudenberg, M.; Galanos, C.; Simon, J. C. Oligosaccharides of Hyaluronan activate dendritic cells via toll-like receptor 4. *J. Exp. Med.* **2002**, *195* (1), 99–111.

(13) Jewell, C. M.; Lynn, D. M. Multilayered polyelectrolyte assemblies as platforms for the delivery of DNA and other nucleic acid-based therapeutics. *Adv. Drug Delivery Rev.* **2008**, *60* (9), 979–999.

(14) Boudou, T.; Crouzier, T.; Ren, K.; Blin, G.; Picart, C. Multiple functionalities of polyelectrolyte multilayer films: new biomedical applications. *Adv. Mater.* **2010**, *22* (4), 441–67.

(15) Best, J. P.; Yan, Y.; Caruso, F. The Role of Particle Geometry and Mechanics in the Biological Domain. *Adv. Healthcare Mater.* **2012**, *1* (1), 35–47.

(16) Yan, Y.; Bjonmalm, M.; Caruso, F. Assembly of Layer-by-Layer Particles and Their Interactions with Biological Systems. *Chem. Mater.* **2014**, *26* (1), 452–460.

(17) De Koker, S.; De Geest, B. G.; Singh, S. K.; De Rycke, R.; Naessens, T.; Van Kooyk, Y.; Demeester, J.; De Smedt, S. C.; Grooten, J. Polyelectrolyte Microcapsules as Antigen Delivery Vehicles To Dendritic Cells: Uptake, Processing, and Cross-Presentation of Encapsulated Antigens. *Angew. Chem., Int. Ed.* **2009**, *48* (45), 8485–8489.

(18) De Geest, B. G.; Willart, M. A.; Lambrecht, B. N.; Pollard, C.; Vervaeke, C.; Remon, J. P.; Grooten, J.; De Koker, S. Surface-Engineered Polyelectrolyte Multilayer Capsules: Synthetic Vaccines Mimicking Microbial Structure and Function. *Angew. Chem., Int. Ed.* **2012**, *51* (16), 3862–3866.

(19) De Koker, S.; Hoogenboom, R.; De Geest, B. G. Polymeric multilayer capsules for drug delivery. *Chem. Soc. Rev.* **2012**, *41* (7), 2867–2884.

(20) Chong, S. F.; Sexton, A.; De Rose, R.; Kent, S. J.; Zelikin, A. N.; Caruso, F. A paradigm for peptide vaccine delivery using viral epitopes encapsulated in degradable polymer hydrogel capsules. *Biomaterials* **2009**, *30* (28), 5178–5186.

(21) Cui, J. W.; De Rose, R.; Best, J. P.; Johnston, A. P. R.; Alcantara, S.; Liang, K.; Such, G. K.; Kent, S. J.; Caruso, F. Mechanically Tunable, Self-Adjuvanting Nanoengineered Polypeptide Particles. *Adv. Mater.* **2013**, *25* (25), 3468–3472.

(22) DeMuth, P. C.; Su, X. F.; Samuel, R. E.; Hammond, P. T.; Irvine, D. J. Nano-Layered Microneedles for Transcutaneous Delivery of Polymer Nanoparticles and Plasmid DNA. *Adv. Mater.* **2010**, *22* (43), 4851–4856.

(23) DeMuth, P. C.; Min, Y. J.; Huang, B.; Kramer, J. A.; Miller, A. D.; Barouch, D. H.; Hammond, P. T.; Irvine, D. J. Polymer multilayer tattooing for enhanced DNA vaccination. *Nat. Mater.* **2013**, *12* (4), 367–376.

(24) Kozlovskaya, V.; Xue, B.; Lei, W.; Padgett, L. E.; Tse, H. M.; Kharlampieva, E. Hydrogen-bonded multilayers of tannic acid as mediators of T-cell immunity. *Adv. Healthcare Mater.* **2015**, *4* (5), 686–94.

(25) Zhang, P.; Chiu, Y. C.; Tostanoski, L. H.; Jewell, C. M. Polyelectrolyte Multilayers Assembled Entirely from Immune Signals on Gold Nanoparticle Templates Promote Antigen-Specific T Cell Response. *ACS Nano* **2015**, *9*, 6465.

(26) Biesheuvel, P. M.; Mauser, T.; Sukhorukov, G. B.; Mohwald, H. Micromechanical theory for pH-dependent polyelectrolyte multilayer capsule swelling. *Macromolecules* **2006**, *39* (24), 8480–8486.

(27) Reddy, S. T.; van der Vlies, A. J.; Simeoni, E.; Angeli, V.; Randolph, G. J.; O'Neil, C. P.; Lee, L. K.; Swartz, M. A.; Hubbell, J. A. Exploiting lymphatic transport and complement activation in nanoparticle vaccines. *Nat. Biotechnol.* **2007**, *25* (10), 1159–64.

(28) Bachmann, M. F.; Jennings, G. T. Vaccine delivery: a matter of size, geometry, kinetics and molecular patterns. *Nat. Rev. Immunol.* **2010**, *10* (11), 787–796.

(29) Neumann, S.; Burkert, K.; Kemp, R.; Rades, T.; Dunbar, P. R.; Hook, S. Activation of the NLRP3 inflammasome is not a feature of all particulate vaccine adjuvants. *Immunol. Cell Biol.* **2014**, *92* (6), 535–542.

(30) Copolovici, D. M.; Langel, K.; Eriste, E.; Langel, U. Cell-penetrating peptides: design, synthesis, and applications. *ACS Nano* **2014**, *8* (3), 1972–94.

(31) Zhang, T. T.; Kang, T. H.; Ma, B.; Xu, Y.; Hung, C. F.; Wu, T. C. LAH4 enhances CD8<sup>+</sup> T cell immunity of protein/peptide-based vaccines. *Vaccine* **2012**, *30* (4), 784–93.

(32) Kanekiyo, M.; Wei, C. J.; Yassine, H. M.; McTamney, P. M.; Boyington, J. C.; Whittle, J. R. R.; Rao, S. S.; Kong, W. P.; Wang, L. S.; Nabel, G. J. Self-assembling influenza nanoparticle vaccines elicit broadly neutralizing H1N1 antibodies. *Nature* **2013**, *499* (7456), 102–106.

(33) Courtney, A. H.; Bennett, N. R.; Zwick, D. B.; Hudon, J.; Kiessling, L. L. Synthetic Antigens Reveal Dynamics of BCR Endocytosis during Inhibitory Signaling. *ACS Chem. Biol.* **2014**, *9* (1), 202–210.

(34) Rosenthal, J. A.; Chen, L. X.; Baker, J. L.; Putnam, D.; DeLisa, M. P. Pathogen-like particles: biomimetic vaccine carriers engineered at the nanoscale. *Curr. Opin. Biotechnol.* **2014**, *28*, 51–58.

(35) Kasturi, S. P.; Skountzou, I.; Albrecht, R. A.; Koutsoukos, D.; Hua, T.; Nakaya, H. I.; Ravindran, R.; Stewart, S.; Alam, M.; Kwissa, M.; Villinger, F.; Murthy, N.; Steel, J.; Jacob, J.; Hogan, R. J.; Garcia-Sastre, A.; Compans, R.; Pulendran, B. Programming the magnitude and persistence of antibody responses with innate immunity. *Nature* **2011**, *470* (7335), 543–7.

(36) Moon, J. J.; Suh, H.; Bershteyn, A.; Stephan, M. T.; Liu, H. P.; Huang, B.; Sohail, M.; Luo, S.; Um, S. H.; Khant, H.; Goodwin, J. T.; Ramos, J.; Chiu, W.; Irvine, D. J. Interbilayer-crosslinked multilamellar vesicles as synthetic vaccines for potent humoral and cellular immune responses. *Nat. Mater.* **2011**, *10* (3), 243–251.